CI&CEQ

Available on line at
Association of the Chemical Engineers of Serbia AChE
www.ache.org.rs/CICEQ

Chemical Industry & Chemical Engineering Quarterly 19 (1) 153–164 (2013) CI&CEQ

SOODABEH KHALILI
ALI ASGHAR GHOREYSHI
MOHSEN JAHANSHAHI

Chemical Engineering Department,
Babol University of Technology,
Babol, Iran

SCIENTIFIC PAPER

UDC 66.081.3:62:54

DOI 10.2298/CICEQ120217050K

CARBON DIOXIDE CAPTURED BY MULTI-WALLED CARBON NANOTUBE AND ACTIVATED CHARCOAL: A COMPARATIVE STUDY

In this study, the equilibrium adsorption of CO_2 on activated charcoal (AC) and multi-walled carbon nanotube (MWCNT) were investigated. Experiments were performed at temperature range of 298-318 K and pressures up to 40 bar. The obtained results indicated that the equilibrium uptakes of CO_2 by both adsorbents increased with increasing pressure and decreasing temperature. In spite of lower specific surface area, the maximum amount of CO_2 uptake achieved by MWCNT at 298 K and 40 bar were twice that of CO_2 capture by AC (15 compared to 7.93 mmol g^{-1}). The higher amount of CO_2 captured by MWCNT can be attributed to its higher pore volume and specific structure of MWCNT, such as hollowness and light mass, which had greater influence than specific surface area. The experimental data were analyzed by means of Freundlich and Langmuir adsorption isotherm models. Following a simple acidic treatment procedure, CO_2 capture was increased marginally by MWCNT over entire range of pressure, while for AC this effect appeared at higher pressures. Small values of isosteric heat of adsorption were evaluated based on Clausius-Clapeyron equation showed the physical nature of adsorption mechanism. The high amount of CO_2 capture by MWCNT renders it as a promising carrier for practical applications such as gas separation.

Keywords: adsorption; CO_2; MWCNT; AC; adsorption isotherms; isosteric heat.

Extensive utilization of fossil fuels has increased CO_2 emission into the atmosphere. Carbon dioxide is one of the major greenhouse gases that may have direct linkage to global climate changes. The control of CO_2 emission is a serious and challenging research topic. Thus, a great deal of efforts has been devoted to limit the emissions of greenhouse gases, especially CO_2, into the environment. For example, CO_2 removal from flue gases at large industrial plants, such as thermal power stations, steal manufacturing plants and oil refineries that use fossil fuel for combustion is considered as a major solution to CO_2 emission problem [1-5].

Correspondence: A.A. Ghoreyshi, Chemical Engineering Department, Babol University of Technology, Babol, Iran.
E-mail: aa_ghoreyshi@nit.ac.ir
Paper received: 17 February, 2012
Paper revised: 17 May, 2012
Paper accepted: 18 May, 2012

Various techniques have been proposed to capture CO_2, including chemical absorption, physical absorption, cryogenic separation, physical adsorption and membrane separation [6-8]. Among them, chemical absorption with aqueous solution of alkanolamines such as monoethanolamine (MEA) and diethanolamine (DEA) has been recognized as the most matured process. However, solvent absorption technology has several disadvantages such as high corrosion, oxidative degradation of absorbents, high-energy consumption for solvent regeneration, high viscosity and foaming in the gas-liquid interface [9, 10]. To overcome these problems, physical adsorption with porous materials has received increasing attention for CO_2 capture from flue gas. Porous media including activated carbon, X-type zeolites, SBA-16 micro-/mesoporous silica sorbents, mesoporous spherical-silica particles and mesoporous molecular sieve MCM-41 are suitable adsorbents for CO_2 capture [11-13].

Among solid adsorbents, carbonaceous materials have been evaluated as potential adsorbents in CO_2 separation. The advantages of carbonaceous materials for CO_2 capture are fast adsorption/desorption kinetics, high surface area, large pore volume and low density that render them as suitable materials for high prersdsure gas adsorption [14,15]. Chandra *et al.* [16] have synthesized N-doped porous carbon produced *via* chemical activation of polypyrrole functionalized graphene sheets and studied the adsorption of CO_2 and N_2 with this adsorbent. Results showed selective adsorption of CO_2 (4.3 mmol g^{-1}) over N_2 (0.27 mmol g^{-1}) at temperature of 298 K and pressure of 1 atm. They have stated that the potential for large scale production and facile regeneration makes this material useful for industrial applications.

Activated carbon is a common adsorbent that is often revealed a good capability in CO_2 capture because of its excellent porous structures, specific surface properties, reusability, minimal costs and environmentally benign nature [17]. Since the emergence of carbon nanotubes (CNTs) in 1991 [18], a series of attempts has been made to evaluate the adsorption properties of these new materials because of their unique properties such as uniform porosity, high pore volume, high specific surface area and low mass density [19]. CNTs have been proven to possess good potential for CO_2 capture from flue gas due to their unique physicochemical properties as well as high thermal and chemical stability [20]. The adsorption of CO_2 in carbonaceous materials such as MWCNT corresponds to the amount of CO_2 adsorption, which takes place near the carbon surface solid only due to the physical forces – van der Waals interactions – that carbon atoms exert on CO_2 molecules. This is the reason why the phenomenon is called physisorption. Lu *et al.* [21] have investigated the adsorption of CO_2 on the raw and 3-aminopropyl-triethoxysilane (APTS)-modified MWCNT, granular activated carbon (GAC), and zeolite at CO_2 concentration range of 5-50%. After the modification, the MWCNT showed the greatest enhancement in adsorption capacity of CO_2, followed by the zeolite and then the GAC.

Recently, pressure swing adsorption (PSA) processes have attracted a great deal of attention as a promising technology for CO_2 capturing due to low cost, high selectivity, high adsorption capacity and easy regeneration of adsorbents [22]. A proper design of a PSA unit requires knowledge of the adsorption isotherms and rate parameters of each adsorbate. Equilibrium parameters are also required as input information to the modeling and simulation of PSA processes. It provides insight about maximum gas storage capacity attainable by a specific adsorbent [23].

The main objective of the present research was to assess the potential of MWCNT as an effective adsorbent for essential capture of CO_2 compared to conventional carbonaceous materials such as AC. Also, the treatment of adsorbents by concentrated acids was evaluated as a way to study the effect of chemical treatment on the structure of adsorbents and amount of CO_2 capture. Experimental results of CO_2 adsorption by these adsorbents at equilibrium state were described by several adsorption isotherm models. The kinetic study was also carried out to evaluate the effectiveness of the adsorption processes. Isosteric heat of adsorption was evaluated from a set of isotherms based on the Clausius-Clapeyron equation. The selected pressure and temperature ranges in this study were based on the effectiveness of the adsorption process. The adsorption of CO_2 on physical adsorbents normally favors lower temperature and higher pressure. Therefore, application of the results of the present study at large industrial plants needs preconditioning of hot flue gas to lower the temperature for effective performance of adsorption plants. However, the pressure range used in the study is typically the operating pressure range at large scale industrial plants (such as pressure swing adsorption PSA plants).

EXPERIMENTAL

Material and its characterization

The MWCNT used in this work were purchased from Alpha Nanotechnologies Company, Ltd. (China), which was synthesized via CVD method with purity greater than 95%. The apparent density of MWCNT was 0.063 g cm^{-1}. The AC used for the measurement of CO_2 adsorption was purchased from Merck Company (Darmstadt, Germany). Apparent density of this adsorbent was 0.2653 g cm^{-1}. Carbon dioxide and helium with purity of 99.99 and 99.995%, respectively, were purchased from Technical Gas Services, UAE. Nitric acid 65% (HNO_3) and sulfuric acid 96% (H_2SO_4) were obtained from Merck.

The materials characterization techniques were applied for each adsorbent. MWCNT was characterized with respect to wall thickness (single or multi-walled), diameter and length by transmission electron microscopy (TEM). Scanning electron microscopy (SEM) was used to obtain supplementary information regarding the MWCNT and AC structure before and after oxidation process.

The pore characteristics for both adsorbents were measured by BET technique employing N_2 adsorption isotherm at 77 K. N_2 adsorption/desorption isotherms were determined at a relative pressure (p/p_0) range of 0.0001-0.99 and used to measure surface area, average pore diameter and pore volume.

Surface characterization of acid treated adsorbents were carried by Fourier transformed infrared spectroscopy (FTIR) spectrometer. Sample discs were prepared by mixing the samples with KBr and scanned in a range from 400 to 4000 cm^{-1}.

Apparatus

The amounts of adsorbed carbon dioxide on the MWCNT and AC, before and after the oxidation process, were determined by volumetric technique. Figure 1 displays the apparatus that was designed to conduct the CO_2 adsorption experiments. The pressure drop due to CO_2 adsorption was measured at constant operating temperature by this apparatus.

The apparatus consisted of two high-pressure cells made of stainless steel, called the pressure and adsorption cell. They were placed in a thermostatic water bath to keep the temperature constant during the CO_2 adsorption. The pressure cell was connected to a regulator and adsorption cell *via* a needle valve to control gas entrance. The gas flew from a CO_2 high-pressure reservoir to the pressure cell *via* the regulator (1) by opening the connecting valve (2). The adsorption experiments were initiated by opening valves 5 and 6 between the pressure cell and adsorption cell and allowing gas entrance to the adsorption cell loaded with the adsorbent. The pressure in the system started to drop as CO_2 was adsorbed on the adsorbents. The equilibrium state was reached when the pressure approached to a constant value. Both cells equipped with a PT100 temperature probe and a pressure transducer that were interfaced to the computer to monitor and record system pressure. The maximum allowable pressure in the installation was 50 bar and its working temperature was in the range of 283-343 K.

In each batch experiment, about 1 g of adsorbent was loaded in an adsorption cell. Prior loading adsorbent into the adsorption cell, the setup was tested against any probable leak using pressurized air for 24 h. Before each test, the adsorbents were degassed at 473 K for 24 h and the system was evacuated by vacuum pump to 0.1 mbar. Helium gas was employed to determine the dead volume by using a calibration cell with a definite volume. By this method the exact volume of pressure and adsorption cell with their connection lines such as tubes and valves were measured.

The amount of adsorbed CO_2 was calculated using material balance before and after each test and SRK equation of state for the compressibility factor:

$$\left.\frac{pV}{ZRT}\right|_{L_1} + \left.\frac{pV}{ZRT}\right|_{a_1} = \left.\frac{pV}{ZRT}\right|_{L_2} + \left.\frac{pV}{ZRT}\right|_{a_2} + N \qquad (1)$$

where subscripts 1, 2, L and a stand for the initial state, final equilibrium state, pressure cell and adsorption cell, respectively; V is the volume, p is the pressure, T is the temperature, R is the universal gas constant, and Z is the CO_2 compressibility factor.

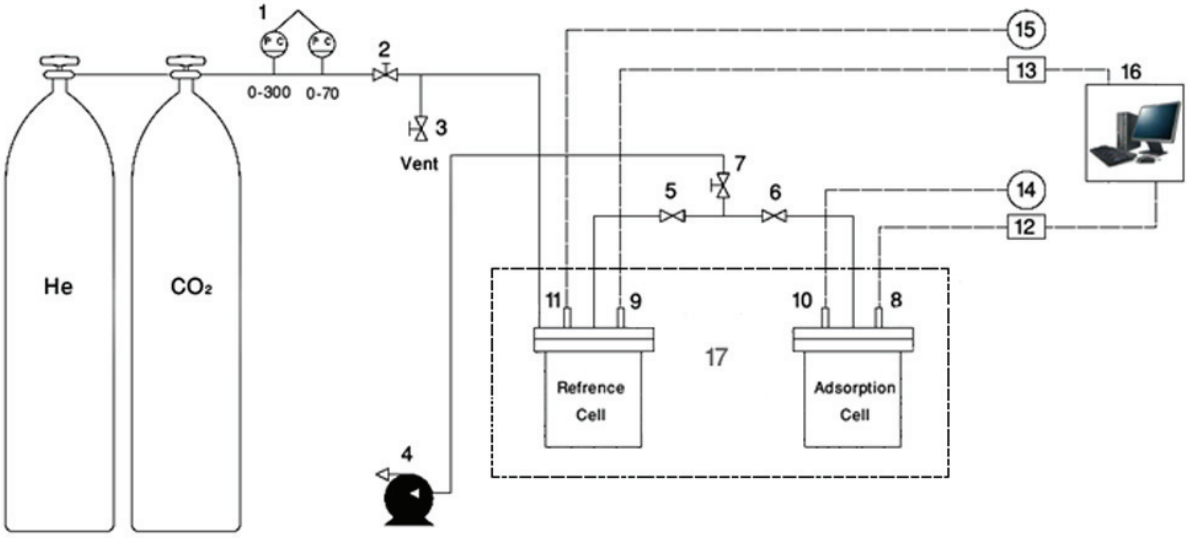

Figure 1. Schematic diagram of the volumetric adsorption apparatus: 1) regulator; 2,3) valves; 4) vacuum pump; 5-7) valves; 8,9) pressure transducer; 10,11) temperature probe; 12,13) pressure digital indicator; 14,15) temperature digital indicator; 16) computer; 17) water bath.

RESULTS AND DISCUSSION

Materials characterizations

The main characteristics such as BET surface area, mean pore diameter and total pore volume have been listed for both adsorbents in Table 1. The specific surface area of AC is about two times of MWCNT, while the MWCNT shows a higher pore volume compared to AC.

Table 1. The structural properties of adsorbents measured by the BET technique

Adsorbent	S_{BET} m^2/g	Pore volume cm^3/g	Mean pore diameter nm
MWCNT	294	0.6231	4.68
AC	545	0.48	3.49

The N_2 adsorption and desorption isotherms at 77 K of the MWCNT and AC are shown in Figure 2. The isotherms were classified as the type II adsorption isotherm defined by IUPAC. Micropores adsorption occurred at the initial part of the curve.

The TEM image of MWCNT is shown in Figure 3a. It was clearly demonstrated that the MWCNT had small amount of catalyst particles (as impurity), but a number of thin amorphous carbon layers sticking to the nanotube walls were observed in some chains of MWCNT. The caps of MWCNT were open, which is important for the gas adsorption because open tubes enable gas adsorption by both the inside and outside of the tubes [24]. The outer diameter of adsorbent ranged from 15 to 20 nm, the inner diameter was about 4 nm, and the length was about 30 μm.

The SEM images for MWCNT before and after acid treatment are shown in Figures 3b and 3c, respectively. It is obvious from Figure 3b that the MWCNT are held together into bundles *via* van der Waals forces and show high degree of aggregation. It was also due to CNT length as the MWCNT showed a larger degree of entanglement [25]. It is clearly demonstrated from Figure 3c that the morphology of MWCNT after oxidation remains undamaged. No destruction and real damage for MWCNT was observed, which indicates that MWCNT is strong enough to withstand during oxidation process. Oxidized MWCNT indicated more obvious ends compared to the pristine MWCNT, because oxidative etching along the walls of MWCNT by strong acids caused the MWCNT to fragment in lengths in the range of 100 to 300 nm. This observation was also reported by the other researchers [26,27].

The porous structure of AC adsorbent is shown in Figure 4a. The existing cavities and cracked structure accounts for high specific surface area of the adsorbent. There are some metal ions and other impurities on the surface of AC. It is obvious from Figure 4b that acid treatment removed impurities on its surfaces. The porosity of COOH-AC was clearer

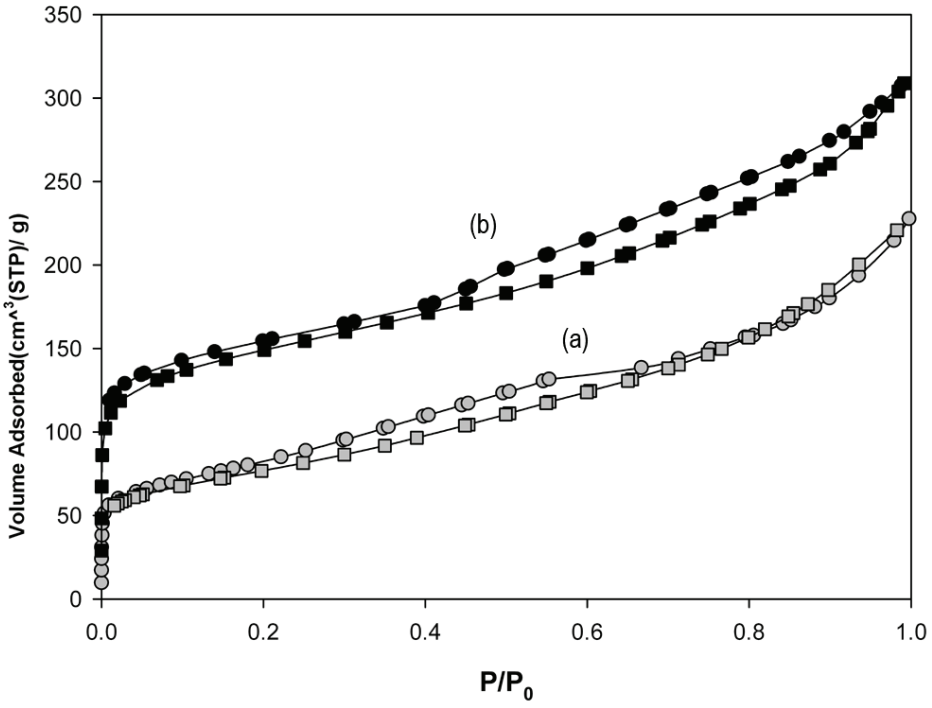

Figure 2. N_2 adsorption/desorption isotherms of MWCNT (a) and AC (b).

than AC because of the destruction of pore walls due to the acid treatment effect. In some cases, the carbon texture was destroyed under oxidative acidic conditions.

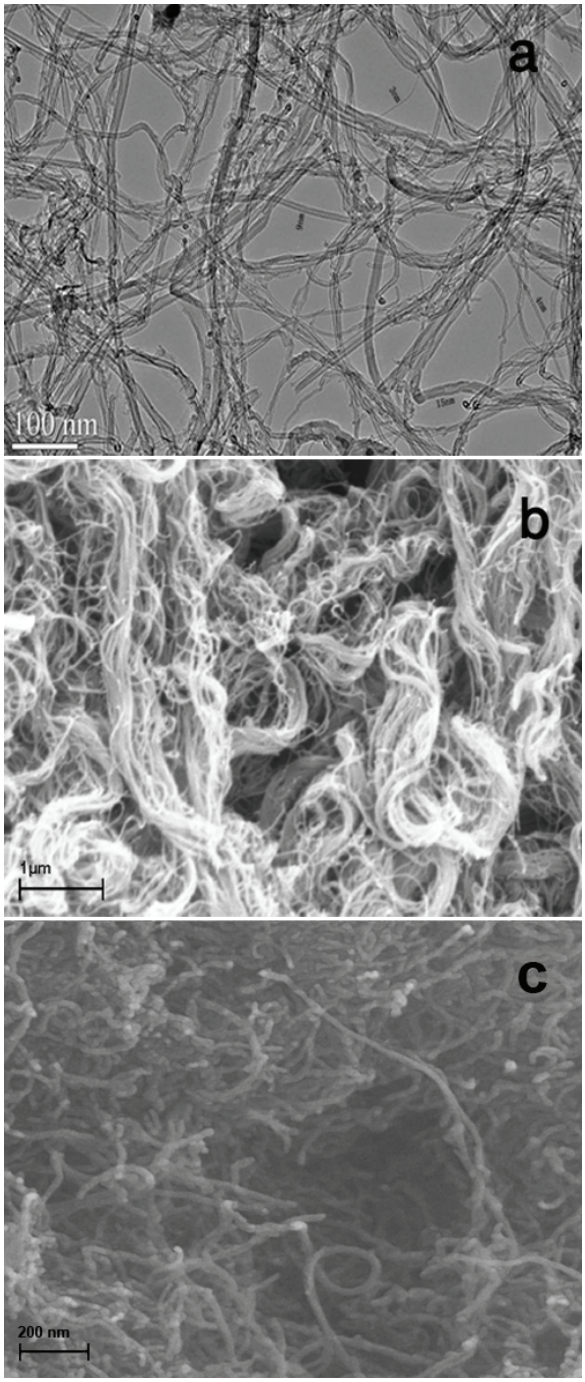

Figure 3. TEM Image of MWCNT (a) and SEM images of MWCNT (b) and COOH-MWCNT (c).

Figure 5 shows the FT-IR spectra of MWNT and AC before and after the oxidation process. The peaks at 1635 and 1627 cm^{-1} are due to the C=C bond of carbon structure of adsorbents. The peaks at 3440 and 3431 cm^{-1} are assigned to the OH band due to water molecules present in the KBr and unmodified adsorbents. After oxidation with strong acids, small peaks at 1714 and 1728 cm^{-1} appeared that belong to the C=O stretching vibration of COOH groups. Asymmetric and symmetric stretching vibrations of C-H are appeared at 2856-2926 cm^{-1} region. Further confirmation of the oxidation process is appearance of C-O band at 1122 and 1224 cm^{-1} and O-H bands at 3440 and 3429 cm^{-1} [28-33].

Acid treatment process

The oxidized MWCNT (COOH-MWCNT) was achieved by adding 100 mg of pristine MWCNTs to 150 ml of mixture of H_2SO_4/HNO_3 (3:1 by volume ration). The mixture was dispersed in an ultrasonic bath for 1 h and then the solution was refluxed at 90 °C for 1 h. After cooling down to room temperature, the solution was filtered with a 0.2 µm cellulose acetate microfiltration membrane and washed with distilled water several times until pH increased to natural. The carboxylated MWCNT was then dried in a vacuum drying oven at 100 °C for 4 h.

Two grams of AC were oxidized with 80 ml of mixture of H_2SO_4/HNO_3 (3:1 by volume ration) at 70 °C for 2 h under magnetic stirring. The oxidized AC (COOH-AC) was filtered, washed with distilled water until natural pH and then dried in a vacuum drying oven at 100 °C for 4 h.

CO_2 adsorption isotherm

The adsorption studies were carried out at different pressures up to 40 bar and three sets of temperatures, *i.e.*, 298, 308 and 318 K. At any given temperature, the amount of CO_2 adsorbed on adsorbents is only a function of pressure. Results demonstrated that CO_2 uptake increased with an increase in pressure and a decrease in temperature. Figure 6 illustrated that the isotherms for AC material lies below those of MWCNT. At higher pressures the adsorption isotherm curve of MWCNT increases almost linearly and it seems that the CO_2 uptake could be continued by increasing pressure, whereas the AC isotherm curve leads to saturation at high pressure. This particular behavior is due to the difference in their structure. Although the specific surface area of AC is much higher than MWCNT and the BET surface area plays an important role in determination of the adsorption capacity, the structure of adsorbent is a key factor in gas adsorption. When AC is exposed to CO_2, gas adsorption occurs in micropores whereas the mesopores and the macropores do not influence the adsorption amount [24,34]. Specific structures of MWCNT such as hollowness and light mass are important in

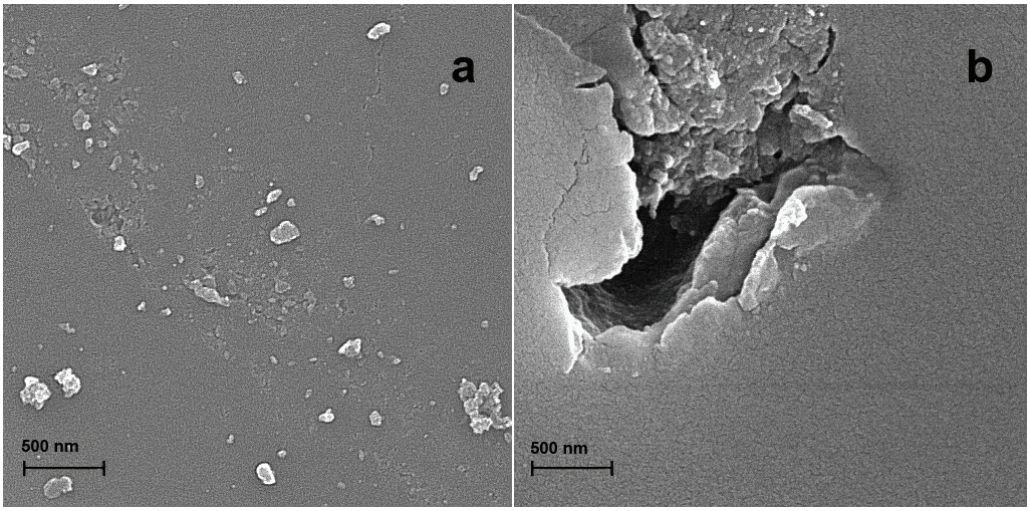

Figure 4. SEM Images of AC (a) and COOH-AC (b).

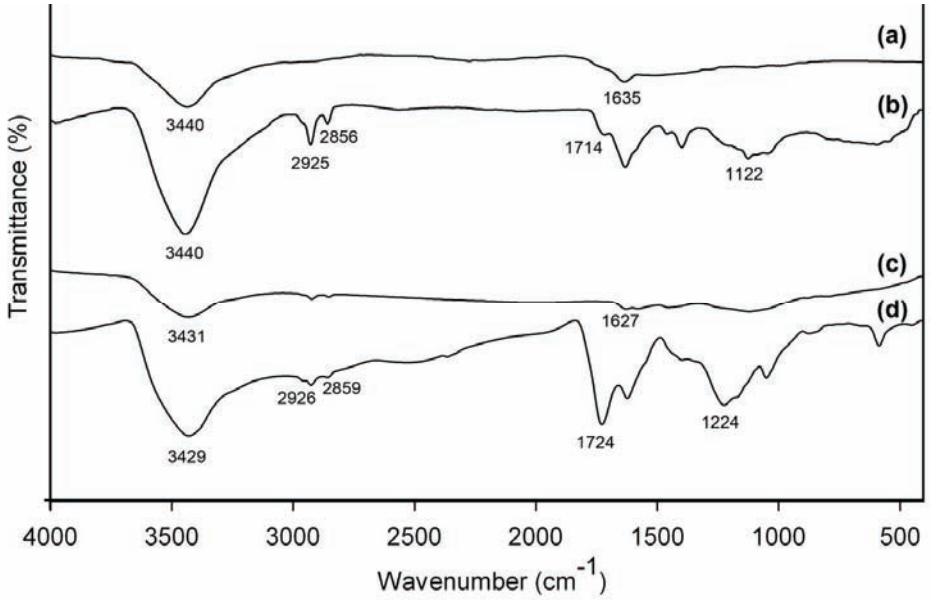

Figure 5. FTIR Spectra of MWCNT (a), COOH-MWCNT (b), AC (c) and COOH-AC (d).

CO_2 adsorption. Actually CO_2 can be stored on the inside area of CNTs, shaping a cylindrical monolayer form, or at the outer surface, or in the interplanar spacing between the adjacent platelets in MWNTs or between the nanotubes in the case of bundles of carbon nanotubes [35].

In this study, at 298 K and 40 bar, the maximum amounts of CO_2 uptake achieved for MWCNT and AC adsorbents were 15 and 7.93 mmol g^{-1}, respectively.

The equilibrium data can be approximated using common and practical adsorption isotherms, which provide the basis for the design of adsorption systems. The amount of adsorbed material onto an adsorbent as a function of its pressure at constant temperature can be described by different adsorption isotherm models. The most famously used isotherm equation for modeling of the adsorption data is the Langmuir equation, which is based on monolayer sorption onto a surface with a finite number of equivalent sites and is given by the following equation [36,37]:

$$q_e = q_m \frac{K_L p}{1 + K_L p} \tag{2}$$

where q_e is the amount of CO_2 adsorbed per unit mass of MWCNT (mmol g^{-1}); q_m is the maximum amount of CO_2 adsorbed (mmol g^{-1}) and K_L is K_L = = k_a/k_b, k_a and k_b are adsorption and desorption constants, respectively.

The Freundlich model is an empirical equation which is used for non ideal sorption on heteroge-

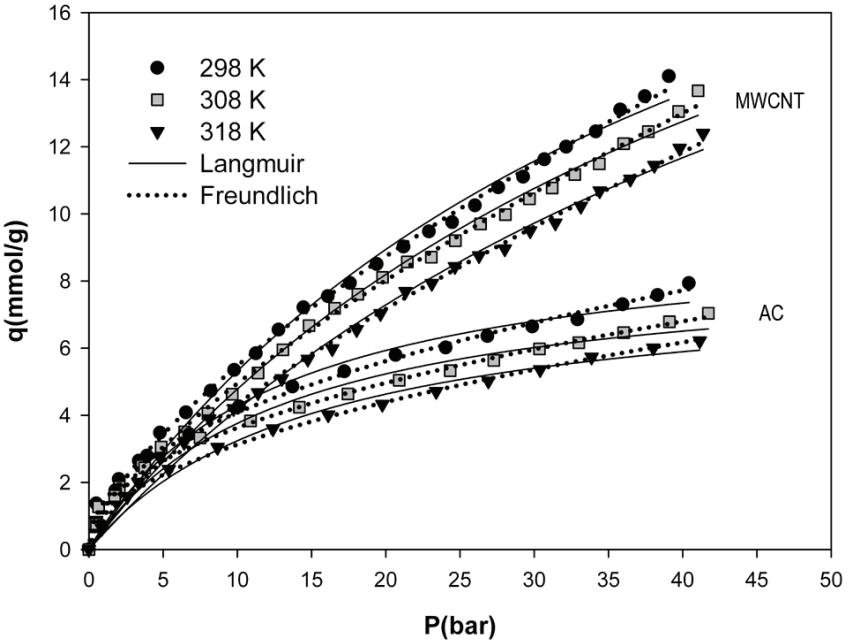

Figure 6. Nonlinear fit of experimental data with Langmuir and Freundlich models.

neous surfaces and it is not restricted to the monolayer sorption [38]. The Freundlich adsorption isotherm is given by the following equation:

$$q_e = K_F p^{\frac{1}{n}} \quad (3)$$

where K_F is Freundlich constant and $1/n$ is the heterogeneity factor. For $n > 1$, adsorption is favorable. The Freundlich isotherm indicates reversible adsorption process [39,40].

The isotherm parameters were obtained through a nonlinear fit of experimental data with isotherm models. Figure 6 shows the comparison of experimental adsorption data to predicted values by Langmuir and Freundlich isotherm models. The values obtained for Langmuir and Freundlich isotherm parameters are shown in Table 2.

The maximum capacity (q_m) of adsorbents and K_L values (Langmuir parameters) for CO_2 adsorption decreased with increasing temperature. These results confirmed that the affinity between CO_2 and adsorbents had an inverse relationship with temperature and indicating an exothermic nature.

It is confirmed by n values higher than 1 in the Freundlich isotherm model that the adsorption is favorable for both adsorbents. Also, the K_F value for both adsorbents decreased with an increase in temperature. This suggests that the adsorption of CO_2 on these adsorbents is more favorable at low temperature, and agreed with the results from Langmuir model [41]. Similar trends were observed in equilibrium adsorption behavior of MWCNT and AC, which indicates a common adsorption mechanism for these carbonaceous materials.

By inspecting the R-squared values (coefficients of determination) for two examined model isotherms (Table 2), Freundlich model has shown a better fit with experimental data than the Langmuir model.

The effect of treatment

The effect of acid treatment on CO_2 adsorption was studied at different pressures up to 40 bars and temperature of 298 K. Figure 7 illustrates the CO_2 adsorption isotherm of acid-treated adsorbents.

The experimental results indicate that the COOH--MWCNT shows improvement compared to pristine

Table 2. Langmuir and Freundlich isotherm constants for adsorption of CO_2 on MWCNT and AC samples

T / K	MWCNT						AC					
	Langmuir			Freundlich			Langmuir			Freundlich		
	q_m	K_L	R^2	K_F	n	R^2	q_m	K_L	R^2	K_F	n	R^2
298	30.81	0.0204	0.9871	1.1103	1.4511	0.9962	9.63	0.0801	0.9842	1.41	2.1720	0.9965
308	28.79	0.0199	0.9918	0.9921	1.4337	0.9977	8.60	0.0775	0.9786	1.27	2.2036	0.9985
318	27.55	0.0180	0.9938	0.8449	1.4025	0.9986	8.11	0.0665	0.9888	1.01	2.0383	0.9969

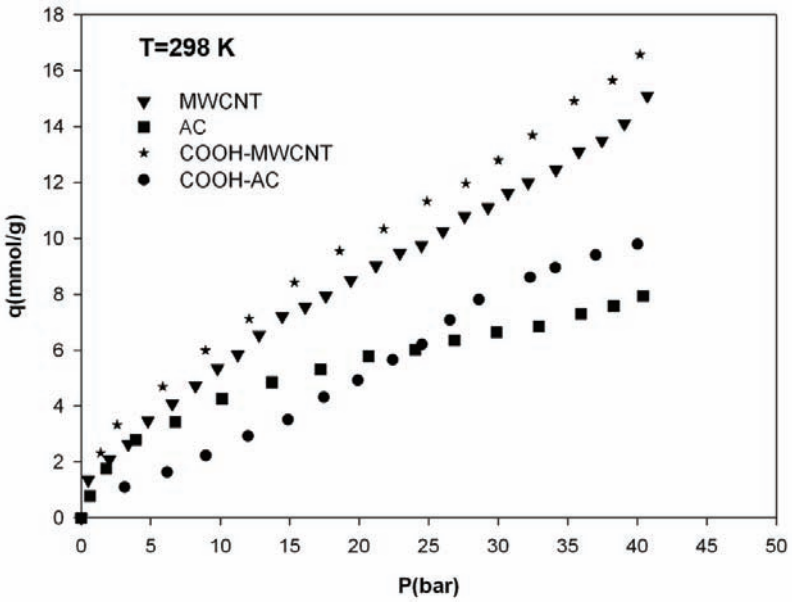

Figure 7. The effect of acid-treated adsorbents in CO_2 capture at 298 K.

MWCNT in CO_2 capture. Acid treatment can eliminate effectively impurities such as the catalyst particles and amorphous carbon. This caused to increase the CNT purity and formation of defects and cavities which originate from removing impurities [35]. Also, chemical modification opened closed-caps of MWCNT, which is useful for gas storage [42]. Nevertheless, the treatments of MWCNT could not have great effects on the CO_2 adsorption capacity (Figure 7), because ends and sidewalls of MWCNT are covered with various oxygen containing groups (mainly carboxyl groups) after pretreatment with concentrated acids, which weakens the adsorption capacity of the nanotubes [43]. Similar trends in equilibrium adsorption behavior of MWCNT and COOH-MWCNT confirms that the morphology of MWCNT remained undamaged after treatment.

From the shape of the isotherms (Figure 7) can be deduced that the adsorption process must in general be different for AC and COOH-AC. The adsorption isotherm for COOH-AC indicates a type IV shape according to IUPAC classification. Micropores adsorption and formation of multilayer film on the pore walls is observed for the initial part of the adsorption isotherm curve. In other words, the adsorption isotherm indicates that the AC has lower microporosity, but higher mesoporosity after chemical modification [1,9]. This fact confirms the destruction of micropore walls as mentioned before. At higher pressures, about 25 bar and up, the amount of CO_2 capture on COOH-AC was higher than for AC. Therefore, if the CO_2 capture at higher pressures is considered, acid treatment of AC could be a way to increase CO_2 capture by this adsorbent. The amounts of CO_2 uptake at 298 K and 40 bar achieved for COOH-MWCNT and COOH-AC adsorbents were 16.57 and 9.79 mmol g^{-1}, respectively.

CO_2 adsorption kinetics

The kinetics of CO_2 uptake by the MWCNT and AC samples at 298 K and about 16 bar were investtigated (Figure 8). The plots of q_t versus t showed that the adsorption kinetics of CO_2 on both adsorbents consisted of two steps – an initial rapid step where adsorption was fast, and a second slow step where equilibrium uptake was obtained.

The recorded data revealed fast kinetics for the adsorption of CO_2 in which most of the adsorption occurs at early time of adsorption experiments and then adsorbent is saturated by the adsorbate. The initial high rate of CO_2 uptake may be attributed to the existence of the vacant active sites and bare surface; however the number of available adsorption sites decreased as the number of CO_2 molecules adsorbed increased. Similar observations were reported in the literature dealing with gas adsorption onto porous adsorbent [44,45]. The equilibrium time was 17 min for MWCNT and 40 min for AC. The relatively fast adsorption of CO_2 on the MWCNT reflected the existence of easier accessibility of adsorption sites for MWCNT than AC [46-49].

Thermodynamic studies

Langmuir and Freundlich isotherms do not give any idea about the adsorption mechanism. Hence, in order to obtain a conceptual understanding of the adsorption mechanism associated with the phenol-

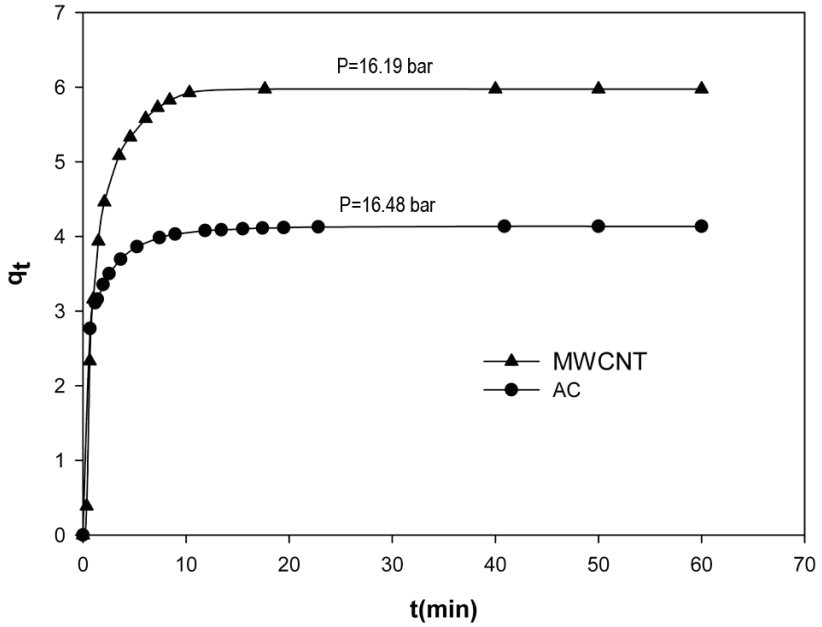

Figure 8. Kinetics of CO_2 adsorption by MWCNT and AC at 298 K.

mena, heat of adsorption was calculated. The heat of adsorption shows the enthalpy change before and after adsorption. Therefore, it is a measure of the strength of interaction between gas molecules and the surface of adsorbent. The isosteric heat of adsorption is defined by the Clausius-Clapeyron equation [50, 51]:

$$\Delta H_{st} = R \frac{d \ln p}{d(1/T)\big|_{q_e}} \quad (4)$$

where p (bar) is pressure at constant equilibrium uptake, R (J mol^{-1} k^{-1}) is the gas constant and T (K) is temperature. The plot of ln p *versus* 1/T gives the isosteric heat of adsorption (Figure 9).

The main difference between physical and chemical adsorption lies in the amount of heat of adsorption. In physical adsorption, the gas molecule is held to the solid surface by weak forces of intermolecular cohesion. The chemical nature of the adsorbed gas remains unchanged; therefore, physical adsorption is a readily reversible process. In chemical adsorption, a strong chemical bond is formed between the gas molecule and adsorbent. Chemical adsorption, or chemisorption, is not easily reversed. Adsorption processes with heat of 80 kJ/mol or more are considered to be controlled by chemisorption, while lower values indicate a physisorption nature of the adsorbent [52,53]. Heat of adsorption for both ad-

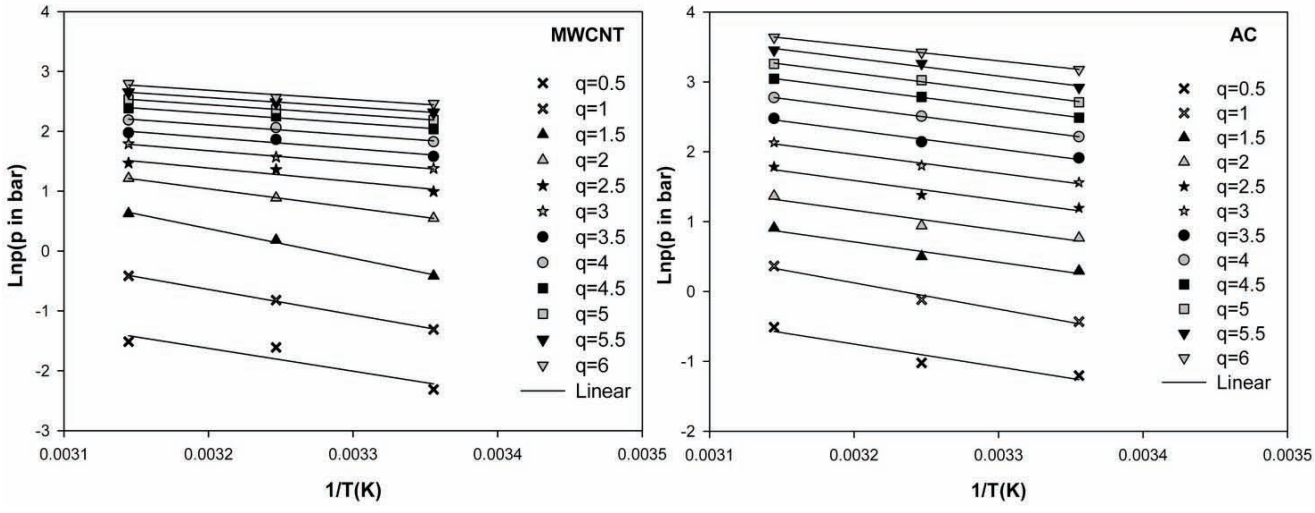

Figure 9. Isosteric heat of adsorption of CO_2 on the MWCNT and AC (q in mmol g^{-1}).

sorbents was much smaller than 80 kJ/mol. This indicates that the process of CO_2 adsorption on the adsorbents used in this study is dominated by physisorption. The negative slopes shown in Figure 10 reconfirmed that the process of adsorption is exothermic.

Figure 10 depicts the variation of the isosteric heat of adsorption with the amount of adsorbed CO_2. At low pressure, the isosteric heat of adsorption increased for both adsorbents. This can be explained by knowing that in lower pressure CO_2 can come into direct contact with the adsorbents due to low surface coverage. This causes a strong interaction between CO_2 and adsorbent surfaces accompanied by high isosteric heat of adsorption. However, at high surface coverage, the weak interaction between CO_2 and adsorbents occurs due to pore filling at high CO_2 equilibrium pressure. Hence, the heat of adsorption decreases.

A comparison between the heat of adsorption of CO_2 on MWCNT and AC revealed that at lower surface cover ages, the heat of adsorption of CO_2 on MWCNT is higher than heat of adsorption of CO_2 on AC. The high heat of adsorption suggests that CO_2 is adsorbed in MWCNT stronger than in AC at low coverage. By increasing surface coverage, this prominence was inversed. At lower surface coverage, the occupation of adsorption sites on MWCNT by CO_2 molecules occurred after AC, which can be attributed to availability of more adsorption sites for CO_2 on MWCNT.

By increasing the surface coverage from 1.5 mmol g^{-1} to more, the isosteric heat of CO_2 adsorption on AC showed a small decrease with the increasing surface coverage (almost constant). The observed small decrease in heat of CO_2 adsorption suggests weak repulsive interactions between adsorbed CO_2 molecules on AC. This phenomenon for MWCNT occurred at almost 4 mmol g^{-1}.

CONCLUSIONS

The adsorption capacity of MWCNT and AC as two potential carbonaceous materials serving as porous media for CO_2 capture was investigated. The experimental isotherm of CO_2 adsorption was determined by the measurement of equilibrium uptake of CO_2 at a pressure range of 0-40 bar at different temperatures. The maximum storage capacity for both materials was obtained at the lowest temperature and highest pressure. The amount of CO_2 adsorbed on MWCNT was almost two times higher than on AC adsorbent, whereas the specific surface area of AC was about two times higher than MWCNT. This can be attributed to the high pore volume, hollowness and lower mass density of MWCNT adsorbent which had stronger impacts on the level of CO_2 loading. Acid treatment increased the amount of CO_2 capture over entire range of pressure for MWCNT without any destruction and real damage on the morphology of MWCNT. For AC, after chemical treatment, the amount of CO_2 capture in comparison to pristine AC increased at higher pressures (25 bar and higher). The kinetics of CO_2 uptake for both samples at 298 K and 16 bar revealed fast adsorption kinetics for both adsorbents, in which most of the adsorption occurred

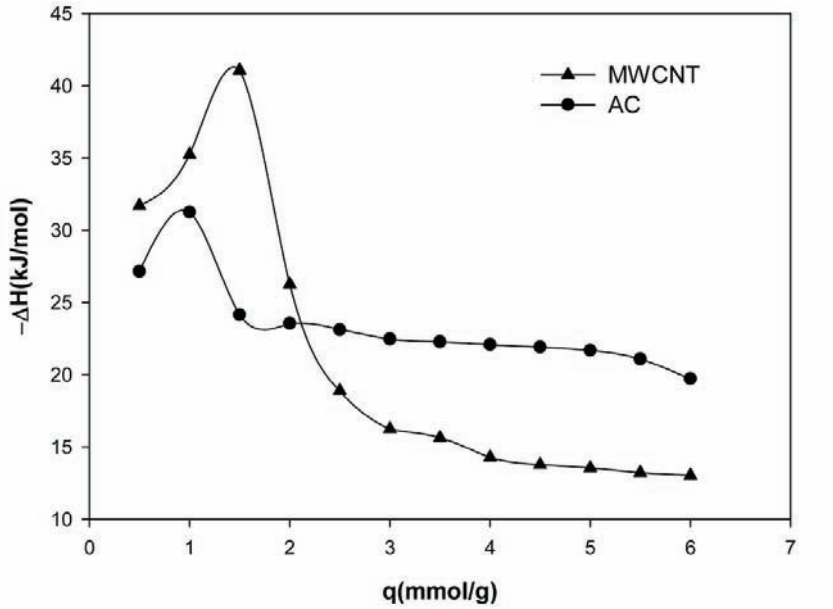

Figure 10. Variation of the isosteric heat of adsorption with the amount of adsorbed CO_2.

in the initial period of adsorption experiments, after which the adsorbents were saturated by the adsorbate. Small values obtained for the isosteric heat of adsorption evaluated from a set of isotherms based on the Clausius-Clapeyron equation indicated the physical nature of adsorption mechanism. The results of the present study indicated that MWCNT seems to be a promising carrier of CO_2 for practical applications. Besides, improved manufacturing technology and large-scale production of CNTs based on CVD method have caused a substantial decrease in its price. This creates a great incentive for development of its application for CO_2 capture purposes.

Nomenclature

Abbreviations

CNTs	Carbon nano tubes
MWCNT	Multi-walled carbon nano tube
AC	Activated charcoal
PSA	Pressure swing adsorption
CVD	Chemical vapor deposition
TEM	Transmission electron microscopy
SEM	Scanning electron microscopy
BET	Brunaner-Emmett-Teller
FTIR	Fourier transformed infrared
IUPAC	International Union of Pure and Applied Chemistry

Symbols

t	Time (min)
p	Pressure (bar)
T	Temperature (K)
V	Volume (cm^3)
Z	Gas compressibility factor
R	Gas constant (bar cm^3 mol^{-1} K^{-1})
q_m	Maximum amount adsorbed (mmol g^{-1})
K_F	Freundlich constant (mmol g^{-1} $bar^{-1/n}$)
ΔH_{st}	Isosteric heat of adsorption (kJ/mol).

REFERENCES

[1] V. Zelenak, D. Halamova, L. Gaberova, E. Bloch, P. Llewellyn, Microporous Mesoporous Mater. **116** (2008) 358--364

[2] C. Chen, W.S. Ahn, Chem. Eng. J. **166** (2011) 646-651

[3] X. Yan, L. Zhang, Y. Zhang, K. Qiao, Z. Yan, S. Komarneni, Chem. Eng. J. **168** (2011) 918-924

[4] G.P. Knowles, J.V. Graham, S.W. Delaney, A.L. Chaffee, Fuel Process. Technol. **86** (2005) 1435-1448

[5] D.J.N. Subagyono, Z. Liang, G.P. Knowles, A.L. Chaffee, Chem. Eng. Res. Des. **89** (2011) 1647-1657

[6] A.A. Olajire, Energy **35** (2010) 2610-2628

[7] R. Chatti, A.K. Bansiwal, J.A. Thote, V. Kumar, P. Jadhav, S.K. Lokhande, R.B. Biniwale, N.K. Labhsetwar, S.S. Rayalu, Microporous Mesoporous Mater. **121** (2009) 84-89

[8] A. Brunetti, F. Scura, G. Barbieri, E. Drioli, J. Membrane Sci. **359** (2010) 115-125

[9] M.R. Mello, D. Phanon, G.Q. Silveira, P.L. Llewellyn, C.M. Ronconi, Microporous Mesoporous Mater. **143** (2011) 174-179

[10] F.Y. Chang, K.J. Chao, H.H. Cheng, C.S. Tan, Sep. Purif. Technol. **70** (2009) 87-95

[11] C. Knofel, J. Descarpentries, A. Benzaouia, V. Zelenak, S. Mornet, P. Llewellyn, V. Hornebecq, Microporous Mesoporous Mater. **99** (2007) 79-85

[12] C. Pevida, M. Plaza, B. Arias, J. Fermoso, F. Rubiera, J. Pis, Appl. Surf. Sci. **254** (2008) 7165-7172

[13] J. Wei, L. Liao, Y. Xiao, P. Zhang, Y. Shi, J. Environ. Sci. **22** (2010) 1558-1563

[14] C.C. Huang, H.M. Chen, C.H. Chen, Int. J. Hydrogen Energy **35** (2010) 2777-2780

[15] D. Saha, S. Deng, Int. J. Hydrogen Energy **34** (2009) 8583--8588

[16] S.U. Yu, S.H. Kim, Y.S. Yoon, D.Y. Kim, A.H. Kwon, M. Meyyappan, K.S. Kim, Chem. Commun. **48** (2011) 735-737

[17] J. Zhu, J. Yang, B. Deng, J. Hazard. Mater. **166** (2009) 866-872

[18] D. Cao, W. Wang, Int. J. Hydrogen Energy **32** (2007) 1939-1942

[19] A. Leela Mohana Reddy, S. Ramaprabhu, Int. J. Hydrogen Energy **33** (2008) 1028-1034

[20] F. Su, C. Lu, W. Cnen, H. Bai, J.F. Hwang, Sci. Total Environ. **407** (2009) 3017-3023

[21] C. Lu, H. Bai, B. Wu, F. Su, J.F. Hwang, Energy Fuels **22** (2008) 3050-3056

[22] M.A. Sheikh, M.M. Hassan, K.F. Loughlin, Gas Sep. Purif. **10** (1996) 161-168

[23] R.K. Motkuri, P.K. Thallapally, B.P. McGrail, S.B. Ghorishi, Cryst. Eng. Comm. **12** (2010) 4003-4006

[24] F.L. Darkrim, P. Malbrunot, G. Tartaglia, Int. J. Hydrogen Energy **27** (2002) 193-202

[25] S.H. Jin, Y.B. Park, K.H. Yoon, Compos. Sci. Technol. **67** (2007) 3434-3441

[26] K. Balasubramanian, M. Burghard, Small **1** (2005) 180-192

[27] D. Tasis, N. Tagmatarchis, V. Georgakilas, M. Prato, Chem. Eur. J. **9** (2003) 4000-4008

[28] S. Murugesan, K. Myers, V.R. Subramanian, Appl. Catal., B **103** (2011) 266-274.

[29] X. Liang, M. Zeng, C. Qi, Carbon **48** (2010) 1844-1848

[30] R. Azzi, E. Denio, D. Ilza, F. Silvio, L. Claudio, M. Rochel, J. Mater. Res. **6** (2003) 1439-1516

[31] S.H. Jin, Y.B. Park, K.H. Yoon, Compos. Sci. Technol. **67** (2007) 3434-3441

[32] G. Vukovic, A. Marinkovic, M. Obradovic, V. Radmilovic, M. Colic, R. Aleksic, P.S. Uskokovic, Appl. Surf. Sci. **255** (2009) 8067-8075

[33] G.D. Vukovic, A.D. Marinkovic, M. Colic, M. Ristic, R. Aleksic, A.A. Peric-Grujic, P.S. Uskokovic, Chem. Eng. J. **157** (2010) 238-248

[34] N. Bagheri, J. Abedi, Chem. Eng. Res. Des. **89** (2011) 2038-2043

[35] G.E. Ioannatos, X.E. Verykios, Int. J. Hydrogen Energy **35** (2010) 622-628

[36] J. He, S. Hong, L. Zhang, F. Gan, Y.S. Ho, Fresenius Environ. Bull. **19** (2010) 2651-2656

[37] Y.H. Huang, C.L. Hsueh, C.P. Huang, L.C. Su, C.Y. Chen, Sep. Purif. Technol. **55** (2007) 23-29

[38] A. Ghaemi, M. Torab-Mostaedi, M. Ghannadi-Maragheh, J. Hazard. Mater. **190** (2011) 916-921

[39] J. Rahchamani, H.Z. Mousavi, M. Behzad, Desalination **267** (2011) 256-260

[40] C.L. Hsueh, Y.W. Lu, C.C. Hung, Y.H. Huang, C.Y. Chen, Dyes Pigm. **75** (2007) 130-135

[41] Q. Fu, Y. Deng, H. Li, J. Liu, H. Hu, S. Chen, T. Sa, Appl. Surf. Sci. **255** (2009) 4551-4557

[42] W. Yulong, W. Fei, L. Guohua, N. Guoqing, Y. Mingde, Mater. Res. Bull. **43** (2008) 1431-1439

[43] F.L. Darkrim, P. Malbrunot, G. Tartaglia, Int. J. Hydrogen Energy **27** (2002) 193-202

[44] N. Azouaou, Z. Sadaoui, A. Djaafri, H. Mokaddem, J. Hazard. Mater. **184** (2010) 126-134

[45] W. Wan Ngah, M. Hanafiah, Biochem. Eng. J. **39** (2008) 521-530

[46] S. Chen, Q. Yue, B. Gao, Q. Li, X. Xu, Chem. Eng. J. **168** (2011) 909-917

[47] A. Kamari, W. Ngah, Colloids Surfaces, B **73** (2009) 257--266

[48] M. Ahmaruzzaman, S. Laxmi Gayatri, Chem. Eng. J. **158** (2010) 173-180

[49] E. Malkoc, Y. Nuhoglu, Sep. Purif. Technol. **54** (2007) 291-298

[50] L. Zhou, Y. Zhou, Y. Sun, Int. J. Hydrogen Energy **29** (2004) 475-479

[51] S.C. Hsu, C. Lu, F. Su, W. Zeng, W. Chen,Chem. Eng. Sci. **65** (2010) 1354-1361

[52] M. Cinke, J. Li, C.W. Bauschlicher, A. Ricca, M. Meyyappan, Chem. Phys. Lett. **376** (2003) 761-766

[53] L.A. Rodrigues, M.L.C.P. da Silva, Desalination **263** (2010) 29-35.

SOODABEH KHALILI
ALI ASGHAR GHOREYSHI
MOHSEN JAHANSHAHI

Chemical Engineering Department, Babol University of Technology, Babol, Iran

NAUČNI RAD

ADSORPCIJA CO_2 NA VIŠESLOJNIM UGLJENIČNIM NANO-CEVIMA I AKTIVNOM UGLJU: KOMPARATIVNA STUDIJA

U ovom radu je ispitivana ravnoteža adsorpcije CO_2 na aktivnom uglju (AC) i višeslojnim ugljeničnim nano-cevima (MVCNT). Eksperimenti su vršeni u temperaturnom opsegu 298-318 K i na pritiscima do 40 bar. Dobijeni rezultati ukazuju da se ravnotežna adsorbovana količina CO_2 od strane oba adsorbenata povećava sa povećanjem pritiska i smanjenjem temperature. Uprkos manjoj specifičnoj površini, maksimalna količina adsorbovanog CO_2 je dva puta veća kod MVCNT na 298 K i 40 bar nego kod AC (15 u poređenju sa 7,93 mmol·g^{-1}). Veća adsorpcije CO_2 od strane MVCNT se može pripisati većoj zapremini pora i specifičnoj strukturi MVCNT, kao što su šupljine i manja mase, koji imaju veći uticaj od specifične površine. Eksperimentalni podaci su analizirani pomoću Freundlich-ovih i Langmuir-ovih adsorpcionih izotermi. Korišćenjem jednostavnog kiselinskog tretmana u celom opsegu datog pritiska neznatno je povećana količina adsorbovanog CO_2 od strane MVCNT, dok se isti efekat kod AC javlja na višim pritiscima. Male vrednosti izosterne toplote adsorpcije određene na osnovu Clausius-Clapeyron-ove jednačine pokazuju fizičku prirodu adsorpcionog mehanizma. Velika adsorbovana količina CO_2 čini MVCNT obećavajućim nosačem za praktične primene, kao što je gasna separacija.

Ključne reči: adsorpcija, CO_2, MWCNT, AC, adsorpcione izoterme, izosterna toplota.